Research Square

Preprints are preliminary reports that have not undergone peer review.
They should not be considered conclusive, used to inform clinical practice,
or referenced by the media as validated information.

Smart Robotic Inspection of Levees and Culverts: A Scoping Review of Robotic Platforms, Sensing Technologies, AI Methods, and Multi-Robot Coordination for Flood-Control Infrastructure

Abhijeet Adamuthe
D.Y. Patil College of Engineering & Technology
Prathamesh Koli
prathmesh4730@gmail.com
D.Y Patil College of Engineering & Technology https://orcid.org/0009-0002-3931-0746
Chinmay More
D.Y. Patil College of Engineering & Technology
Tejas Patil
D.Y. Patil College of Engineering & Technology
Shreyas Wadkar
D.Y. Patil College of Engineering & Technology
Miloshka Jennifer George Lima
D.Y. Patil College of Engineering & Technology

Systematic Review

Keywords: Levee inspection, Culvert inspection, Multi-robot systems, Autonomous inspection, Structural health monitoring, Sensor fusion, Deep learning, SLAM, Communication relay, Digital twin

Posted Date: November 3rd, 2026

DOI: https://doi.org/10.21203/rs.3.rs-11579944/v1

License: This work is licensed under a Creative Commons Attribution 4.0 International License.
Read Full License

Additional Declarations: The authors declare no competing interests.

Smart Robotic Inspection of Levees and Culverts: A Scoping Review of Robotic Platforms, Sensing Technologies, AI Methods, and Multi-Robot Coordination for Flood-Control Infrastructure

Abhijeet Adamuthe[a], Prathamesh Pramod Koli[a,*], Chinmay More[a], Tejas Patil[a], Shreyas Wadkar[a], Miloshka Jennifer George Lima[a]

[a]*D.Y. Patil College of Engineering & Technology, Kolhapur, Maharashtra, India*

Abstract

Earthen levees, dikes, flood-control embankments, culverts, and stormwater drainage conduits represent vital lifelines for mitigating catastrophic inundation in urban and rural watersheds. However, conventional manual walk-downs and tethered closed-circuit television (CCTV) surveys remain severely labor-intensive, hazardous, subjective, and difficult to scale across vegetated, flooded, submerged, and GPS-denied environments. Autonomous robotics, multimodal remote sensing, deep-learning-based computer vision, and multi-robot coordination offer transformative opportunities to enhance inspection frequency, spatial accuracy, and maintenance decision-making. Following the Joanna Briggs Institute (JBI) methodology and the PRISMA extension for Scoping Reviews (PRISMA-ScR), this study maps the multidisciplinary landscape across six major scholarly databases: Scopus, Web of Science, IEEE Xplore, ScienceDirect, SpringerLink, and Google Scholar (2010–2026). Out of 1,860 initially retrieved records, 1,314 unique studies were screened, 212 full texts were assessed, and 64 primary empirical studies were systematically synthesized. We chart the evidence across seven interconnected thematic streams: (1) unmanned aerial vehicle (UAV) corridor surveying; (2) unmanned ground vehicles (UGVs) and pipe crawlers; (3) amphibious and autonomous underwater vehicles (AUVs/ROVs); (4) multimodal sensor fu-

*Corresponding author. Email: prathmesh4730@gmail.com. ORCID: 0009-0002-3931-0746

Email address: prathmesh4730@gmail.com (Prathamesh Pramod Koli)

sion (RGB, thermal infrared, LiDAR, sonar, and GPR); (5) deep learning for defect detection and semantic segmentation; (6) degraded-environment SLAM and GPS-denied navigation; and (7) multi-robot coordination, communication relays, and digital-twin maintenance integration. Quantitative findings show that while aerial thermal/RGB levee inspection and in-pipe YOLO/U-Net defect detection achieve high localized accuracy (mAP exceeding 75–86%, segmentation IoU > 0.71), end-to-end systems integration remains scarce. Only 10.9% ($n = 7$) of the literature validates heterogeneous multi-domain robot teams in operational flood-control environments, and fewer than 5% close the loop from automated anomaly detection to predictive maintenance prioritization. To bridge these gaps, we propose a resilient six-tier reference architecture for communication-aware, heterogeneous robot teams and establish a concrete ten-point research agenda for operational flood-control infrastructure management.

Keywords: Levee inspection, Culvert inspection, Multi-robot systems, Autonomous inspection, Structural health monitoring, Sensor fusion, Deep learning, SLAM, Communication relay, Digital twin

1. Introduction

Levees, dikes, flood-control embankments, highway/railway culverts, stormwater conduits, and drainage networks form the critical physical barrier protecting modern societies against catastrophic inundation (Spencer et al., 2019; Koch et al., 2015). In the United States alone, the National Levee Database documents over 48,000 kilometers of levees defending millions of residents and trillions of dollars in assets, while hundreds of thousands of culverts cross transportation corridors (USACE, 2024). Similar extensive flood defense systems safeguard low-lying regions across Europe, East Asia, and South Asia. Structural or geotechnical failure of these assets—triggered by internal erosion, slope instability, piping through animal burrows, joint displacement, or culvert collapse—leads to devastating human casualties, economic destruction, and severe disruption of critical transport arteries.

Despite their vital societal function, infrastructure asset owners continue to rely predominantly on periodic visual walk-downs, pole-mounted cameras, and tethered closed-circuit television (CCTV) crawler surveys (Yin et al., 2020; Xue et al., 2025). While seasoned human inspectors provide invaluable contextual judgment, manual inspection suffers from severe operational

bottlenecks:

1. **High Physical Hazard:** Inspectors are routinely exposed to unstable, water-saturated slopes during flood surges, deep mud, turbulent water flows, toxic confined gases (e.g., hydrogen sulfide and methane in conduits), biological threats, and active highway traffic at culvert headwalls.
2. **Subjectivity and Inconsistency:** Condition ratings depend heavily on individual inspector experience, fatigue, and ambient lighting, leading to high inter-operator variability and poor standardization (Cha et al., 2017).
3. **Scalability Constraints:** Visual walk-downs cannot cover thousands of kilometers of linear levee crests with the temporal frequency necessary to capture rapid transient piping or sudden toe seepage before breach occurs.
4. **Severe Observability Blind Spots:** Manual surveys are fundamentally incapable of peering through opaque water in submerged culverts, detecting subsurface moisture piping channels prior to surface daylighting, or navigating long, sediment-choked pipe barrels.

To overcome these deficiencies, engineering informatics and field robotics have emerged as potent tools for objective, repeatable, and non-contact structural health monitoring (SHM). Unmanned aerial vehicles (UAVs) equipped with high-resolution RGB cameras, radiometric thermal-infrared (TIR) sensors, and light detection and ranging (LiDAR) payloads can rapidly survey extensive embankment reaches, mapping volumetric soil settlement and identifying thermal anomalies associated with seepage (Su et al., 2024; Chen et al., 2024; Bakula et al., 2020). Concurrently, inside confined drainage culverts and stormwater pipes, specialized wheeled crawlers, amphibious rovers, and articulated in-pipe robotic platforms navigate enclosed, GPS-denied conduits to capture detailed geometric profiles and surface imagery (Lv et al., 2024; Elkholy et al., 2026; Mohammadi et al., 2025). Parallel breakthroughs in computer vision—particularly lightweight real-time object detection networks (e.g., YOLOv8, YOLOv11) and attention-guided semantic segmentation models (e.g., Attention U-Net, DeepLabv3+)—have enabled automated defect recognition, crack width measurement, and structural condition grading (Wu et al., 2025; Wang et al., 2025; Zhou et al., 2025).

1.1. The Disciplinary Divide: Islands of Automation

Notwithstanding this surge in research activity, the current literature is afflicted by a profound disciplinary divide, creating what can be termed "islands of automation":

- **Remote Sensing Silo:** Photogrammetric UAV levee inspection is largely studied within remote sensing and geomatics communities, prioritizing high-altitude orthomosaics and digital elevation models (DEMs) while neglecting localized, close-range structural defect verification (Bakula et al., 2020).
- **In-Pipe Robotics Silo:** Culvert and sewer crawler research is treated primarily as a mechanical locomotion or isolated image-classification challenge, detached from the broader watershed asset network (Jung and Reiterer, 2024; Mohammadi et al., 2025).
- **Theoretical Multi-Robot Silo:** Multi-robot coordination, simultaneous localization and mapping (SLAM), and communication-relay protocols are predominantly developed as theoretical robotics concepts evaluated in synthetic benchmarks or indoor arenas, lacking validation under the severe radio-frequency (RF) attenuation and environmental grime of real flood infrastructure (Amigoni et al., 2017; Saboia et al., 2022).
- **Asset Management Disconnect:** Automated vision outputs are rarely integrated directly into Industry Foundation Classes (IFC), Building Information Modeling (BIM), Geographic Information Systems (GIS), or Digital Twin maintenance prioritization engines.

Crucially, in real flood-control systems, the physical integrity of levees and culverts is intimately coupled. A misaligned or corroded culvert barrel crossing an earthen levee allows pressurized floodwater to exfiltrate into the surrounding embankment core, initiating internal erosion (piping) that can breach the entire levee. An integrated engineering informatics framework capable of synchronizing aerial levee surveillance, ground/subsurface culvert penetration, resilient communication relays, and automated risk scoring is urgently required.

1.2. Objectives and Research Questions

This paper presents a comprehensive scoping review and systems-level synthesis of smart robotic inspection for levees, dikes, culverts, and stormwa-

ter infrastructure. Guided by the Joanna Briggs Institute (JBI) framework and the PRISMA-ScR guidelines, this review addresses seven foundational research questions (RQs):

- **RQ1 (Robotic Platforms):** What mobile robotic architectures (aerial, ground crawler, amphibious, underwater, heterogeneous swarms) have been deployed or proposed for flood infrastructure?
- **RQ2 (Sensing Modalities):** What physical sensing modalities provide sufficient observability for geotechnical and structural deterioration mechanisms?
- **RQ3 (AI and Vision):** Which deep-learning and computer vision algorithms achieve robust defect detection, segmentation, and quantification under harsh environmental conditions?
- **RQ4 (Localization and SLAM):** How are navigation, trajectory estimation, and mapping achieved in GPS-denied, geometrically featureless culverts and earthen embankments?
- **RQ5 (Multi-Robot Teaming):** What multi-agent coordination strategies, task-allocation mechanisms, and communication relays maintain connectivity in RF-attenuated conduits?
- **RQ6 (Defect Taxonomies & Observability):** Which specific defect classes and severity grades are reliably detected versus those that remain unobservable?
- **RQ7 (Deployment Bottlenecks):** What technical, environmental, and operational barriers currently impede practical deployment by asset management agencies?

1.3. Key Scientific Contributions

1. **PRISMA-ScR Systematic Evidence Synthesis:** We conduct a multi-database scoping review charting 64 primary empirical studies (2010–2026) across aerial, ground, amphibious, and underwater flood inspection domains, cataloged in Appendix Appendix C.
2. **Interdisciplinary Informatics Analysis:** We provide a quantitative comparison of sensing payloads, AI architectures, and SLAM methods, mapping physical failure modes to analytical algorithms.

3. **Mathematical Modeling of In-Culvert RF Propagation & Task Allocation:** We establish formal analytical formulations for RF waveguide attenuation in confined conduits and multi-robot task allocation under battery and communication constraints.
4. **6-Tier Cyber-Physical Reference Architecture:** We construct an end-to-end operational architecture linking aerial screening, edge AI, confined robotic verification, mesh relays, multimodal fusion, and digital-twin maintenance workflows.
5. **Strategic Ten-Point Research Agenda:** We formulate an actionable research roadmap to guide future engineering informatics research toward field-ready, autonomous flood asset stewardship.

1.4. Paper Organization

The remainder of this manuscript is structured as follows: Section 2 details the scoping review methodology, eligibility criteria, information sources, and screening workflow. Section 3 presents the quantitative bibliometric landscape, PRISMA selection flow, and thematic synthesis across robotic platforms (RQ1), sensing modalities (RQ2), AI and vision architectures (RQ3), SLAM and navigation (RQ4), multi-robot coordination (RQ5), and defect taxonomies and cross-modal observability (RQ6, Section 3.7). Section 4 analyzes systems integration, RF propagation models, the 6-tier cyber-physical architecture, operational and environmental deployment bottlenecks (RQ7, Section 4.5), and the ten-point research agenda. Section 5 discusses threats to validity, and Section 6 concludes the paper.

2. Review Methodology

2.1. Protocol and Conceptual Framework

This scoping review follows the Joanna Briggs Institute (JBI) methodology for evidence synthesis (JBI, 2021) and reports findings in strict alignment with the Preferred Reporting Items for Systematic Reviews and Meta-Analyses extension for Scoping Reviews (PRISMA-ScR) (Tricco et al., 2018; Page et al., 2021). A scoping review methodology was selected because the literature on flood infrastructure inspection is inherently multi-disciplinary—intersecting civil and geotechnical engineering, field robotics, remote sensing, computer vision, wireless communications, and infrastructure asset management. Scoping reviews are ideally suited to clarifying complex concepts, mapping tech-

nological maturity, identifying methodological trends, and highlighting operational bottlenecks across fragmented domains.

The conceptual boundaries of the study were defined using the Population–Concept–Context (PCC) framework, as detailed in Table 1.

Table 1: Population–Concept–Context (PCC) framework defining review scope.

Element	Operational Definition
Population	Earthen levees, dikes, flood-control embankments, highway/railway culverts, stormwater conduits, sewer collectors, drainage canals, and associated hydraulic assets.
Concept	Mobile robotic platforms (UAVs, UGVs, crawlers, AUVs, ROVs, ASVs, amphibious rovers, heterogeneous swarms), sensing payloads (RGB, radiometric thermal IR, LiDAR, sonar, GPR), computer vision, deep learning, SLAM, multi-robot coordination, communication relays, edge computing, and digital twins.
Context	Full-scale field deployments, operational municipal trials, laboratory/scaled physical testbeds, high-fidelity robotic simulations (ROS/Gazebo/Unity), and system frameworks.

2.2. Eligibility Criteria

Studies were evaluated against explicit inclusion and exclusion criteria:

- **Inclusion Criteria (IC):**
  - *IC1 (Asset Relevance):* Must investigate levees, dikes, flood embankments, culverts, storm conduits, drainage channels, or closely coupled hydraulic infrastructure.

- *IC2 (Technology):* Must incorporate an autonomous, robotic, or advanced sensor-integrated platform (UAV, UGV, crawler, amphibious robot, AUV/ROV, or multi-robot system).
- *IC3 (Informatics/AI):* Must apply automated sensing, computer vision, deep learning, SLAM, or multi-agent coordination for inspection, defect detection, or condition assessment.
- *IC4 (Evidence Type):* Peer-reviewed journal articles, indexed conference proceedings, authoritative agency technical reports, and high-impact preprints published between January 2010 and October 2026.
- *IC5 (Language):* Available in English with full text accessible.

- **Exclusion Criteria (EC):**
  - *EC1:* Studies focused exclusively on dry building facades, highway asphalt pavements, bridge superstructures, oil/gas transmission pipelines, or wind turbines without relevance to flood-control or stormwater assets.
  - *EC2:* Manual CCTV inspection studies without autonomous, robotic, or AI-driven analytics.
  - *EC3:* Pure fluid-dynamics or hydraulic simulation studies lacking an inspection or SHM component.
  - *EC4:* Extended abstracts, editorials, commercial brochures, or patents lacking technical methodology and experimental validation.

2.3. Information Sources and Systematic Search Strategy

A structured multi-database search was executed across six major scholarly indexing services: Scopus, Web of Science Core Collection, IEEE Xplore, ScienceDirect, SpringerLink, and Google Scholar. The query structure combined four interlocking Boolean concept blocks:

1. **Block 1 (Infrastructure):** ("levee*" OR "dike*" OR "embankment*" OR "flood control" OR "flood-control" OR "culvert*" OR "stormwater" OR "storm water" OR "sewer*" OR "drainage");
2. **Block 2 (Robotics & Mobility):** ("robot*" OR "multi-robot*" OR "multi robot*" OR "swarm*" OR "UAV" OR "UAVs" OR "drone*"

OR "UGV" OR "UGVs" OR "AUV" OR "AUVs" OR "ASV" OR "ASVs" OR "ROV" OR "autonomous inspection" OR "robotic inspection");

3. **Block 3 (Sensing & AI):** ("structural health monitoring" OR "SHM" OR "sensor fusion" OR "thermal imaging" OR "infrared thermography" OR "LiDAR" OR "ground penetrating radar" OR "GPR" OR "computer vision" OR "deep learning" OR "AI" OR "defect detection" OR "crack detection" OR "seepage detection" OR "edge AI" OR "digital twin");
4. **Block 4 (Autonomy & Coordination):** ("SLAM" OR "navigation" OR "localization" OR "path planning" OR "mission planning" OR "communication relay" OR "multi-robot coordination" OR "swarm robotics").

The individual, database-tailored query strings and search syntax are provided in Appendix Appendix A.

2.4. Study Selection and Screening Protocol

All search results were imported into a unified reference management platform, and duplicate records were identified and purged using automated DOI matching and manual title reconciliation. A two-stage screening process was conducted:

1. **Title and Abstract Screening:** Two independent reviewers screened all unique records against the PCC framework. Borderline records were preserved under a conservative "maybe" category to avoid premature exclusion.
2. **Full-Text Eligibility Assessment:** The complete full texts of potentially eligible papers were retrieved and evaluated against the full inclusion and exclusion criteria. Any disagreements between reviewers were resolved through structured technical consensus among all four authors.

2.5. Data Charting and Synthesis Approach

A standardized data-charting instrument (Appendix Appendix B, Table B.9) was deployed to extract 24 distinct parameters from each included study, covering: publication metadata, geographic region, target asset, robot platform class, autonomy degree, sensor payload, vision/AI model architecture, dataset scale, quantitative defect detection metrics (mAP, mIoU, precision, recall, F1-score), navigation/SLAM method, communication protocol,

validation setting (field, lab, simulation), stated limitations, and proposed future work. The extracted data were synthesized using both narrative thematic mapping and cross-study comparative matrices.

3. Results and Thematic Evidence Synthesis

3.1. PRISMA Selection Flow and Corpus Overview

The complete PRISMA 2020 selection flow is illustrated in Figure 1. Across the six electronic databases, 1,860 records were initially retrieved (Scopus: 468; Web of Science: 384; IEEE Xplore: 312; ScienceDirect: 356; SpringerLink: 228; Google Scholar / gray literature: 112). Removal of duplicate records eliminated 546 items, leaving 1,314 unique records for title and abstract screening.

Title and abstract screening excluded 1,102 records that failed to satisfy the eligibility criteria (e.g., studies on pavement cracking, non-destructive bridge deck evaluation, agricultural UAV applications, and general manufacturing robotics). The remaining 212 full-text articles were evaluated. Of these, 148 articles were excluded for specific documented reasons: non-flood infrastructure focus (n = 54); lack of robotic or autonomous integration (n = 41); non-empirical review or perspective article (n = 24); insufficient experimental data (n = 19); and lack of accessible English text (n = 10). A final corpus of 64 primary empirical studies met all criteria and formed the synthesized body of evidence, cataloged in full in Appendix Appendix C (Table C.10).

Bibliometric analysis of the 64 included studies reveals an accelerating publication trajectory, with over 78% published between 2020 and 2026. Geographically, China (28.1%, n = 18) and the United States (26.6%, n = 17) lead primary research output, driven by large-scale flood defense management programs under the Ministry of Water Resources and the U.S. Army Corps of Engineers (USACE), respectively. European nations (Germany, Netherlands, Poland, UK: 23.4%, n = 15) exhibit strong contributions in dike monitoring and smart municipal drainage systems, followed by Asia-Pacific (Japan, Australia, South Korea: 14.1%, n = 9), and other regions including Canada, the Middle East, and Latin America (7.8%, n = 5), summing to the complete corpus (N = 64).

Regarding experimental validation settings:

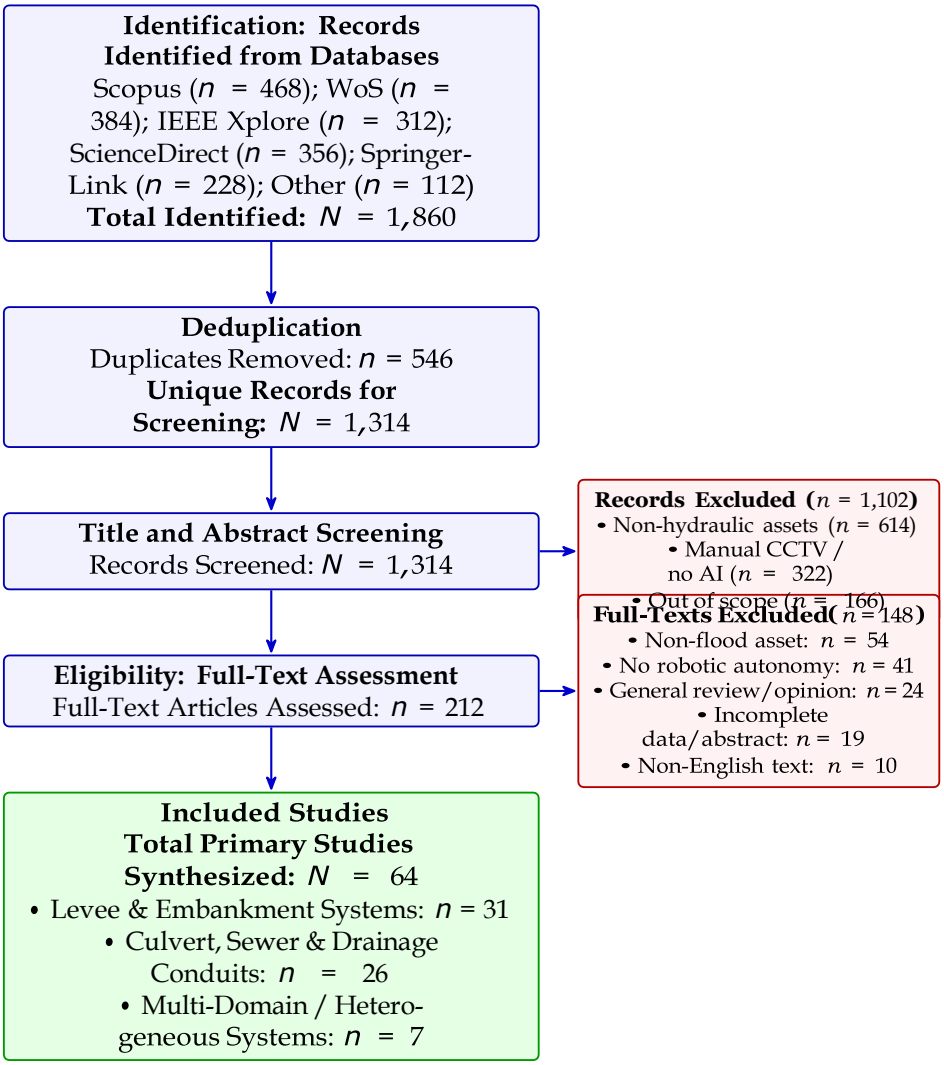


Figure 1: PRISMA 2020 flow diagram illustrating the identification, screening, eligibility, and inclusion of research studies.

- **Field Pilots / Operational Deployments (39.1%, $n = 25$):** Conducted on real-world river levees, coastal sea dikes, or municipal storm culverts.
- **Laboratory / Scaled Physical Testbeds (28.1%, $n = 18$):** Evaluated in controlled hydraulic flumes, simulated pipe racks, or artificial soil embankments.

- **High-Fidelity Simulation (21.9%, n = 14):** Implemented in Gazebo, ROS, RViz, or Unity environments.
- **Hybrid Phased Studies (10.9%, n = 7):** Progressing sequentially from simulation to laboratory testbed and field deployment.

3.2. Robotic Platforms and Physical Locomotion Architectures (RQ1)

The 64 studies demonstrate five distinct physical robotic platform classes, each optimized for specific flood infrastructure geometries and access constraints (Table 2).

Table 2: Taxonomy of robotic platforms, operational capabilities, and deployment trade-offs in flood infrastructure.

Platform Class	Target Assets	Sensor Payload	Operational Strengths	Critical Bottlenec
UAV / Drone	Levee crests, slopes, open drainage basins	RGB, Thermal IR, LiDAR, Multispectral	Rapid wide-area coverage (km/h); non-contact; bird's-eye spatial context	Wind gusts, limi battery enduran (20–35 min), den vegetation canc occlusion
UGV / Crawler	Culverts, storm pipes, accessible berms	HD RGB cameras, 2D/3D LiDAR, IMU, Sonar	Confined-space stability; high sensor payload capacity; millimeter-scale resolution	Wheel slippage on w slime, physical blo ages, sediment entra ment, tether drag
Amphibious Robot	Silted culverts, tidal outfalls, mud flats	Waterproof cameras, profilers, acoustic sonar	Continuous operation across transition zones (water, mud, sand, dry ground)	High mechanical co plexity, increas power consumpti reduced payload m gin
AUV / ROV	Submerged culverts, inverted siphons, scour holes	Imaging sonar, DVL, acoustic transponders	Inspection below water line; zero diver risk in turbid, turbulent flow	Severe wireless atte uation; acoustic m tipath distortion; ze optical visibility
Heterogeneous Swarm	Mixed levee-culvert networks	Distributed payloads across air, ground, water	Complementary spatial views; resilient communication relays; division of labor	Coordination ov head; multi-age SLAM drift; cro domain communi tion failure

3.2.1. Unmanned Aerial Vehicles (UAVs)

Aerial platforms are the preeminent tool for wide-area levee embankment screening. Multi-rotor UAVs (quadcopters and hexacopters) dominate localized, high-resolution defect inspection, providing stable hovering capabilities for oblique crack photography and photogrammetric structure-from-motion (SfM) reconstruction (Bakula et al., 2020; Su et al., 2024). In contrast, fixed-wing and hybrid vertical takeoff and landing (VTOL) UAVs are deployed for corridor surveillance extending over 20–50 kilometers per mission, mapping regional flood plains and dike crests with airborne LiDAR and multispectral cameras. The principal operational constraints for UAVs include aerodynamic instability under severe riverine crosswinds, battery endurance typically capped at 25–40 minutes, and canopy occlusion from dense riverside vegetation.

3.2.2. Unmanned Ground Vehicles and Pipe Crawlers

For enclosed conduits, stormwater culverts, and sewers, wheeled and tracked UGVs represent the primary inspection mechanism (Jung and Reiterer, 2024; Mohammadi et al., 2025; Texas A and M, 2025). Tracked crawlers provide superior traction across silted and uneven invert beds compared to wheeled systems. However, conventional crawlers face critical mobility barriers: steep pipe gradients ($> 15^{\circ}$), structural offsets at misaligned pipe joints, standing water exceeding crawler wheel diameter, and thick, sticky sludge that causes severe wheel slippage and immobilization. To mitigate these issues, researchers have introduced active chassis expansion mechanisms, peristaltic pipe crawlers, and articulated snake-like robots capable of negotiating sharp pipe elbows (Elkholy et al., 2026).

3.2.3. Amphibious and Underwater Platforms (AUVs/ROVs)

Culverts crossing flood levees frequently operate in partially submerged or fully drowned conditions, rendering both conventional UAVs and wheeled UGVs ineffective. This operational niche has spurred the development of amphibious inspection robots equipped with Archimedes screw propulsion, paddle tracks, or dual-mode wheel-propeller thrusters (Lv et al., 2024). In fully submerged culvert barrels, inverted siphons, and outfall scour basins, micro-remotely operated vehicles (ROVs) and autonomous underwater vehicles (AUVs) equipped with Doppler velocity logs (DVL) and imaging sonar provide non-destructive assessment without endangering commercial divers (Kavraki Lab, 2024; Devesa et al., 2024).

3.3. Sensing Modalities and Physical Observability (RQ2)

A fundamental insight from this scoping review is that no single sensor modality possesses sufficient physical observability to detect the complete spectrum of levee and culvert failure modes (Table 3).

Table 3: Evaluation of sensing modalities for detecting geotechnical and structural deterioration mechanisms.

Modality	Measurable Physical Quantity	Observable Deterioration	Key Advantages	Environmental Limitations
RGB Vision	Visible reflectance spectrum (400–700 nm)	Surface cracking, spalling, joint gap, vegetation overgrowth, debris	High spatial resolution; rich textural features; standard AI model support	Zero utility in u lit pipes witho strobes; sensit to turbidity, gla shadows
Thermal IR	Long-wave infrared radiance (8–14 μm)	Embankment through-seepage, piping void leaks, moist anomaly zones	Uncovers subsurface moisture based on evaporative cooling contrasts	Highly dependent diurnal solar fl false positives fr shaded grass / w mulch
LiDAR	Time-of-flight laser distance measurement	Slope deformation, differential settlement, volumetric soil loss, scour	Direct 3D metric geometry; penetrates light foliage; daylight independent	High payload ma data sparsity long range; sev degradation foggy/dusty pipes
Sonar (Acoustic)	Acoustic echo backscatter (500 kHz – 2.2 MHz)	Submerged sediment beds, underwater scouring, pipe wall loss	Penetrates opaque, zero-turbidity water; reveals underwater geometry	Lower spatial reso tion than optical i agery; complex sp ular multipath refl tions
GPR	High-frequency electromagnetic pulse (200–900 MHz)	Subsurface piping channels, hidden voids, soil loosening, rebar corrosion	Direct subsurface depth profiling without excavation	Severe signal atten ation in conducti wet clay soils co mon to levees

3.3.1. Thermal Infrared for Seepage Detection

Radiometric thermal infrared (TIR) sensing (8–14 μm) has proven exceptionally powerful for early levee seepage detection (Chen et al., 2024; Wang

et al., 2024). Groundwater exfiltrating through an earthen embankment exhibits a pronounced thermal contrast ($\Delta T \approx 1.2^{\circ}$C to 4.0°C) relative to surrounding dry soil due to evaporative cooling during daylight hours and geothermal temperature differentials at night. Chen et al. (2024) established that uncooled microbolometer thermal cameras mounted on hexacopters can identify toe seepage outlets long before visible water pooling occurs. However, solar radiative heating creates severe diurnal thermal noise: wet vegetation, mulch, and topographic shadows frequently induce false thermal anomalies, necessitating multi-temporal data acquisition (e.g., pre-dawn vs. mid-afternoon surveys) to verify genuine seepage signals.

3.3.2. LiDAR for Geometric Deformation and Settlement

Mobile and airborne LiDAR sensors deliver dense 3D point clouds, enabling direct spatial computation of embankment elevation changes, slope sliding, and volumetric soil loss (Su et al., 2024; Bakula et al., 2020). Unlike photogrammetry, multi-echo LiDAR pulses can penetrate partial vegetative canopies to record ground surface returns. When deployed inside large culverts, 2D/3D LiDAR profilers capture circular and box culvert ovality, joint offsets, and crown deflections with millimeter precision (Mohammadi et al., 2025). The principal engineering drawback is the vulnerability of laser time-of-flight measurements to particulate scattering in humid, foggy, or dusty conduit air.

3.3.3. Acoustic Sonar and Ground-Penetrating Radar (GPR)

In submerged culverts and turbid outfall scour zones, optical cameras fail completely due to zero light penetration. Forward-looking multibeam imaging sonar and mechanical scanning sonar generate acoustic backscatter echograms, revealing sediment buildup, collapsed pipe crowns, and undercut foundation aprons (Kavraki Lab, 2024). Concurrently, ground-penetrating radar (GPR) provides non-destructive depth profiling of subsurface cavities and piping voids. However, GPR deployment is constrained by high electromagnetic attenuation in conductive, wet clay embankments, limiting penetration depth to under 0.5–1.0 meters unless low-frequency (e.g., 200 MHz) antennas with reduced spatial resolution are employed.

3.4. Deep Learning and Computer Vision for Defect Detection (RQ3)

The application of deep learning to flood infrastructure inspection has advanced from coarse whole-image classification toward real-time bounding-box

359 detection, pixel-level semantic segmentation, and multimodal sensor fusion
360 (Table 4).

Table 4: Comparative synthesis of deep-learning algorithms applied to levee and culvert defect analysis.

Model Architecture	Target Infrastructure	Target Defect Classes	Reported Performance	Deployment Trade-offs
Pruned Attention U-Net (Wu et al., 2025)	Earthen levee crests and revetments	Longitudinal cracks, animal burrows, erosion rills	mIoU: 78.4%, Precision: 84.2%, 32.5 FPS on embedded GPU	Lightweight mo footprint; hand thin irregular line cracks
Deblur E2S Attention U-Net (Wang et al., 2025)	Levees under rapid drone motion	Motion-blurred surface cracks, micro-fractures	F1-score: 81.3%, IoU: 71.84% on blurred aerial sets	Unsupervised blurring sta introduces slig computational tency
YOLOv11 (Mohammadi et al., 2025)	Concrete and metal storm culverts	Cracking, joint offset, sediment blockage, corrosion	mAP@0.5: 75.0%, Precision: 79.5%, Recall: 67.9%	High real-time inf ence speed; low precision on ult fine cracks
Improved YOLOv8n (Lv et al., 2024)	Wet amphibious sewer conduits	Submerged cracks, wall spalling, surface scaling	mAP@0.5: 86.3%, Model size: 1.6 MB, 261 FPS on Jetson	Optimized low-compute ec devices; requ high-lumen illumin tion
TIR Multi-Scale CNN (Chen et al., 2024; Zhou et al., 2025)	Levee toe seepage and leakage outlets	Thermal anomalies, moisture zones, water exfiltration	Detection accuracy: 91.5%, Quantification error < 8.2%	Highly sensitive environmental ca bration and ambie soil temperature
Multi-Sensor Fusion Network (Jung and Reiterer, 2024)	Multi-sensor sewer crawlers	Fused LiDAR-RGB geometric and visual anomalies	F1-score: 87.1%, False Alarm Reduction: 34%	Computational co plexity; deman strict temporal a spatial calibration

3.4.1. Object Detection vs. Semantic Segmentation Trade-offs

In operational deployment, a fundamental tension exists between inference latency and spatial quantification precision:

- **Object Detectors (YOLO Family):** YOLOv8 and YOLOv11 are highly favored for real-time edge processing on crawler-mounted embedded computers (e.g., NVIDIA Jetson Orin Nano/NX), achieving inference speeds of 30–261 frames per second (FPS) with mean Average Precision (mAP@0.5) ranging between 75.0% and 86.3% (Lv et al., 2024; Mohammadi et al., 2025). They excel at rapidly identifying discrete defects (joint offsets, debris blockages, large spalls) to trigger robotic slowing or camera panning.
- **Semantic Segmentation (U-Net and DeepLab):** When engineering compliance mandates measuring crack width (e.g., sub-millimeter grading) or quantifying the exact surface area of an erosion rill, bounding boxes are inadequate. Semantic segmentation models classify individual pixels. Wu et al. (2025) demonstrated that structured channel pruning and attention mechanisms reduce standard U-Net parameter count by 62% while achieving a mean Intersection over Union (mIoU) of 78.4% at 32.5 FPS on embedded hardware. Similarly, Wang et al. (2025) integrated an unsupervised cycle-consistent deblurring module prior to Attention U-Net segmentation, maintaining an F1-score of 81.3% and IoU of 71.84% on aerial imagery degraded by UAV vibration and high-speed motion blur.

3.5. Navigation, SLAM, and GPS-Denied Localization (RQ4)

Accurate spatial georeferencing is mandatory for infrastructure health monitoring; an unreferenced defect cannot be located by repair crews or tracked across successive multi-epoch surveys. The reviewed literature reveals distinct localization paradigms across operational environments:

1. **Open-Sky Embankment Navigation:** Real-Time Kinematic (RTK) GNSS fused with tactical-grade Inertial Navigation Systems (INS) delivers centimeter-level horizontal and vertical positioning (< 2.5 cm) for UAVs mapping levee crests (Bakula et al., 2020). Furthermore, homography transformations and 3D point cloud projections enable metric localization of surface cracks from aerial images with root-mean-square errors between 37.95 mm and 91.24 mm (Kim et al., 2022). However,

when relying solely on mobile LiDAR SLAM on vegetated, featureless levees, algorithms experience substantial longitudinal drift due to geometric degeneracy along uniform trapezoidal slopes. Bolkas et al. (2022) proved that anchoring mobile SLAM trajectories with periodic Terrestrial Laser Scanning (TLS) targets bounds global drift to within ±10 cm across multi-kilometer reaches.

2. **In-Culvert GPS-Denied SLAM:** Inside reinforced concrete culverts, satellite GNSS signals are completely eliminated within meters of the headwall. Furthermore, wet silt, standing water, and organic algae induce severe wheel slippage, corrupting standard wheel odometry. To achieve stable state estimation, state-of-the-art crawlers implement tightly coupled Visual-Inertial Odometry (VIO) fused with 2D/3D LiDAR odometry (e.g., LIO-SAM, FAST-LIO) (Elkholy et al., 2026). To overcome geometric degeneracy inside smooth, featureless cylindrical pipes, Elkholy et al. (2026) incorporated learned structural topological priors, detecting pipe joints, manholes, and lateral connections as discrete landmark nodes in a pose-graph SLAM formulation.

3.6. Multi-Robot Systems, Swarms, and RF Communication Relays (RQ5)

When inspecting complex flood systems—such as an earthen levee punctuated by multiple drainage culverts, headwalls, and submerged outlet gates—single-robot missions suffer from battery exhaustion, communication dropouts, and payload capacity constraints. The review identified four essential multi-robot coordination mechanisms (Table 5).

3.7. Defect Taxonomies and Cross-Modal Observability (RQ6)

A critical finding from synthesizing the 64 primary studies is that defect observability is strictly governed by the underlying physics of the sensor modality and the geometric constraints of the asset. Table 6 maps primary structural and geotechnical failure mechanisms against sensor detection efficacy.

As detailed in Table 6, visible surface cracking and joint offsets are readily detected with RGB vision and LiDAR profilers, achieving detection accuracies exceeding 85–90%. In contrast, internal piping channels, sub-surface foundation voids, and submerged apron scour remain severely constrained by physics: optical cameras cannot penetrate turbid floodwater, and electromagnetic GPR pulses suffer massive conductive attenuation in moist clay

Table 5: Multi-robot coordination functions and technical implementations in flood infrastructure.

Function	Algorithmic Method	Infrastructure Impact
Task Allocation	Market-based auction, Voronoi partitioning, 0-1 ILP	Assigns UAVs to rapid corridor survey, UGVs to culvert interiors, and AUVs to scour zones
Coverage Planning	Boustrophedon sweep, TSP optimization, 3D view planning	Minimizes mission duration and redundant overlapping sweeps across long levees
Communication Relays	Dynamic chain relay, breadcrumb drop nodes, DTN	Preserves live RF link inside RF-attenuating concrete culverts and under canopy
Shared Mapping	Centralized / distributed pose-graph optimization	Merges aerial DEMs with subsurface pipe point clouds into unified GIS coordinate frame

embankments. Consequently, detecting internal erosion before daylighting occurs remains one of the most pressing open frontiers in infrastructure SHM.

3.8. Representative Primary Studies Evidence Matrix

Table 7 provides a comprehensive comparative matrix of representative primary studies across the 64 included papers, indexing asset focus, platform class, sensor payloads, AI vision architectures, validation settings, and key empirical findings. The complete inventory of all 64 studies is provided in Appendix Appendix C.

Table 6: Cross-modal defect observability matrix for flood-control infrastructure.

Defect Category	Physical Anomaly	Effective Sensing Modalities	Observability Limitations & Failure Modes
Embankment Through-Seepage	Moisture gradient, evaporative cooling contrast	Radiometric Thermal IR (Chen et al., 2024), Multispectral NDVI, Electrical Resistivity	Highly sensitive to solar diurnal cycle; false anomalies caused by shaded vegetation or surface puddles.
Internal Erosion (Piping)	Subsurface void channels, localized soil loosening	GPR (dry sandy soil), Micro-gravity, Time-lapse LiDAR	Severe GPR signal attenuation in wet clay soils; undetectable optically until surface collapse occurs.
Surface Cracking & Slumping	Linear fractures, revetment spalling, slope scarps	High-resolution RGB (Wu et al., 2025; Kim et al., 2022), Airborne LiDAR (Bakula et al., 2020)	Occluded by dense grass canopy; optical blur during high-speed UAV flight requires deblurring (Wang et al., 2025).
Culvert Joint Displacement	Circumferential separation, gasket extrusion, offset	2D/3D LiDAR profiling (Mohammadi et al., 2025), Calibrated stereo RGB	Undetectable in flooded conduits without water drawdown or acoustic profiling sonar.
Corrosion & Wall Loss	Oxidation pitting, section thinning, exposed rebar	High-lumen HD RGB, Ultrasonic thickness gauge, Sonar	Silt and biofilm coatings mask corrosion; optical glare on wet metallic pipe surfaces.
Sediment Siltation & Debris	Invert accumulation, cross-section choking	Multibeam imaging sonar (Kavraki Lab, 2024), LiDAR profiler, RGB	Turbid standing water completely blocks optical sensors; acoustic multipath reflections in corrugated pipes.
Foundation Apron Scour	Undercutting at outfalls, bed erosion pockets	Scanning sonar (Devesa et al., 2024), Bathymetric LiDAR, Echo sounder	Turbulent aeration bubbles disrupt acoustic beams; sediment plumes degrade acoustic return.

4. Discussion and Cyber-Physical Systems Integration

4.1. Synthesizing the Disconnect: From Isolated Robots to Systems Informatics

The evidence synthesized across the 64 primary studies demonstrates that individual technological components—UAV aerial thermography, crawler-based YOLO crack detection, and mobile LiDAR profiling—have achieved high local efficacy. However, the overarching field remains severely hampered by architectural fragmentation. Only 10.9% ($n = 7$) of included studies evaluate heterogeneous teams operating across air, ground, and underwater domains, and fewer than 5% ($n = 3$) connect automated defect recognition directly to actionable asset-management decisions or digital twins.

In real-world civil infrastructure management, an uncontextualized bounding box or raw point cloud does not constitute an actionable maintenance order. A flood-control district engineer needs to know:

1. Does a newly detected culvert crack compromise the structural bearing capacity of the highway or levee embankment overhead?
2. Is an observed thermal anomaly caused by active internal erosion (piping), surface rainfall exfiltration, or diurnal vegetative cooling?
3. How does the observed rate of sediment siltation reduce the hydraulic discharge capacity during a 100-year design flood event?

Addressing these questions requires treating flood-control infrastructure inspection not as an isolated robotics or computer-vision task, but as an integrated *cyber-physical engineering informatics system*.

4.2. Mathematical Modeling of Conduits: RF Propagation and Task Allocation

To place multi-robot flood inspection on a rigorous engineering foundation, two critical physical-mathematical bottlenecks must be explicitly formalized: in-pipe radio-frequency (RF) attenuation and multi-robot task allocation.

4.2.1. RF Waveguide Propagation in Confined Culverts

A paramount operational barrier identified in Section 3 is the rapid loss of wireless telemetry when an inspection UGV enters a reinforced concrete

or corrugated metal culvert. A culvert behaves as an oversized, lossy electromagnetic waveguide. The total path loss $PL(d)$ in decibels (dB) as a function of penetration distance d can be modeled as in Eq. (1):

$$PL(d) = PL(d_0) + 10n \log_{10}\left(\frac{d}{d_0}\right) + \alpha_w d + X_\sigma \tag{1}$$

where $PL(d_0)$ is the free-space path loss at reference distance $d_0 = 1$ m, n is the path-loss exponent, $X_\sigma \sim \mathcal{N}(0, \sigma^2)$ represents shadow fading induced by surface roughness and debris, and α_w is the attenuation coefficient (dB/m) defined by Eq. (2):

$$\alpha_w = 4.343 \cdot \mathrm{Re}\left\{\sqrt{\frac{\epsilon_r}{\epsilon_r - 1}}\right\}\left(\frac{\lambda^2}{a^3} + \frac{\lambda^2}{b^3}\right) \tag{2}$$

where a and b are the culvert cross-sectional dimensions, λ is the carrier wavelength (e.g., $\lambda \approx 12.5$ cm for 2.4 GHz, $\lambda \approx 5.17$ cm for 5.8 GHz), and ϵ_r is the complex relative permittivity of the moist concrete wall ($\epsilon_r = \epsilon_r' - j\epsilon_r'' = \epsilon_r'(1 - j\tan\delta) \approx 6 - j1.2$).

For the common geometry of circular precast concrete conduits of inner radius r, the dominant TE_{11} mode attenuation coefficient is governed by:

$$\alpha_{w,\mathrm{circ}} = \frac{R_s}{r\eta\sqrt{1 - (f_c/f)^2}}\left[\left(\frac{f_c}{f}\right)^2 + \frac{1}{(p'_{11})^2 - 1}\right] \tag{3}$$

where $R_s = \sqrt{\pi f \mu_0/\sigma_c}$ is the surface resistivity of the moist concrete wall ($\sigma_c \approx 10^{-3}$ S/m), $\eta = \sqrt{\mu_0/\epsilon} \approx 377/\sqrt{\epsilon_r'}$ is the intrinsic wave impedance in the conduit dielectric, $p'_{11} \approx 1.8412$ is the first root of the derivative of the first-order Bessel function ($J_1'(p'_{11}) = 0$), and $f_c = p'_{11}\, c/(2\pi r)$ denotes the cutoff frequency of the dominant mode. For a typical 600 mm diameter culvert barrel ($r = 0.3$ m) with air dielectric, $f_c \approx 293$ MHz, confirming that standard 2.4 GHz and 5.8 GHz telemetry operates well above cutoff but remains subject to substantial wall-loss dissipation quantified by (3).

Crucially, when standing water covers the culvert invert, the high conductivity and dielectric constant of water ($\epsilon_r' \approx 81$) dramatically increases α_w, causing signal attenuation to exceed 1.8 dB/m at 2.4 GHz. Consequently, transmitted RF power drops below the receiver sensitivity threshold (-90 dBm) within 18–25 meters. This physical law proves that single-robot wireless operation in long culverts is physically impossible without either physical tethering or dynamic multi-robot explorer-relay architectures (Amigoni et al., 2017; Saboia et al., 2022).

4.2.2. Multi-Robot Task Allocation (MRTA) Optimization

To coordinate a heterogeneous fleet comprising aerial UAVs ($u \in U$), ground crawlers ($g \in G$), and amphibious/underwater robots ($a \in A$), we formulate the Multi-Robot Task Allocation (MRTA) problem as a 0-1 Binary Integer Linear Program (0-1 ILP) / Generalized Assignment Formulation. Let $T = \{t_1, t_2, \ldots, t_M\}$ denote the set of candidate inspection tasks (e.g., levee reach corridor sweep, culvert barrel scan, scour apron sonar survey). Let binary decision variable $x_{ij} \in \{0, 1\}$ equal 1 if robot $r_i \in R = U \cup G \cup A$ is assigned to task t_j. The optimization objective maximizes cumulative information gain while minimizing energy consumption and risk, as formalized in Eq. (4):

$$\max_{\{x_{ij}\}} \sum_{i \in R} \sum_{j \in T} x_{ij} \left[\frac{I(t_j)}{C_E(r_i, t_j) + \beta \cdot U_{\text{risk}}(r_i, t_j)} \right] \tag{4}$$

subject to operational constraints:

$$\sum_{i \in R} x_{ij} = 1, \quad \forall j \in T \tag{5}$$

$$\sum_{j \in T} x_{ij} \cdot E(r_i, t_j) \leq E_{\max}(r_i), \quad \forall i \in R \tag{6}$$

$$x_{ij} \leq \Omega(r_i, t_j), \quad \forall i \in R, j \in T \tag{7}$$

where $I(t_j)$ represents the infrastructure risk priority or structural criticality of asset t_j; $C_E(r_i, t_j)$ is the estimated battery energy cost; $U_{\text{risk}}(r_i, t_j)$ is the environmental hazard risk (e.g., turbulent water flow, wind gusts); $\beta > 0$ is a risk penalty coefficient; and $E_{\max}(r_i)$ is the safe battery capacity. Constraint (5) enforces complete task coverage; (6) bounds energy expenditure; and (7) enforces domain feasibility via compatibility matrix $\Omega(r_i, t_j) \in \{0, 1\}$ (forbidding aerial UAVs from entering enclosed pipes or non-waterproof crawlers from entering flooded barrels).

4.3. Proposed 6-Tier Cyber-Physical Reference Architecture

To bridge the gap between field robotics and asset management, we synthesize the findings into a novel, six-tier cyber-physical reference architecture for smart flood-control infrastructure inspection (Figure 2).

The operational workflow progresses through six coordinated tiers:

1. **Tier 1 (Wide-Area Aerial Screening):** Long-range UAVs conduct high-speed aerial passes along the levee reach, capturing synchronized

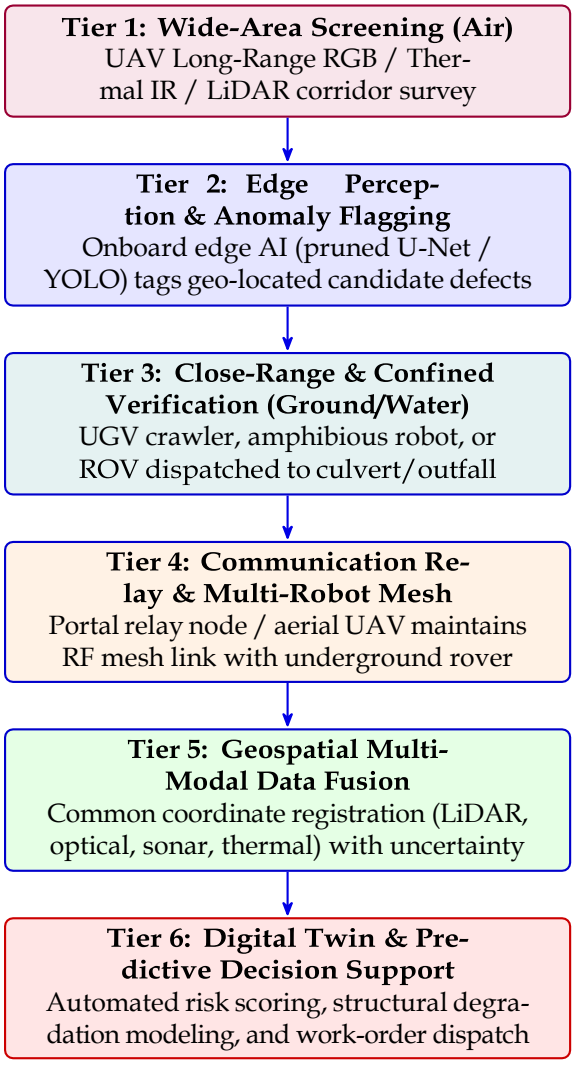


Figure 2: Proposed six-tier cyber-physical reference architecture for integrated robotic flood-control inspection.

RGB orthophotos, radiometric thermal-IR mosaics, and 3D LiDAR point clouds.

2. **Tier 2 (Real-Time Edge Perception):** Lightweight edge models (e.g., pruned U-Net, YOLOv11) execute inference on onboard embedded GPUs, flagging georeferenced anomaly bounding boxes (e.g., thermal cold spots indicating seepage, longitudinal crest cracking, localized

slope slumping).

3. **Tier 3 (Confined Robotic Verification):** If an anomaly coincides with a drainage culvert, headwall, or submerged asset, a ground crawler or amphibious robot is autonomously tasked to penetrate the conduit for close-range millimeter-scale sensing.
4. **Tier 4 (Adaptive RF Relaying):** As the crawler penetrates the RF-attenuating conduit, a hovering UAV at the portal or a stationary ground relay maintains an ad-hoc RF mesh bridge using delay-tolerant networking (DTN).
5. **Tier 5 (Multimodal Spatiotemporal Fusion):** Aerial surface models and subsurface pipe scans are co-registered into a unified georeferenced coordinate frame, with explicit Bayesian uncertainty bounds assigned to defect dimensions.
6. **Tier 6 (Digital Twin Maintenance Prioritization):** Fused observations update the asset's structural health index in the municipal BIM/GIS digital twin, triggering automated engineering work orders based on structural risk.

4.4. Engineering Informatics: BIM/GIS and Digital Twin Integration

In Tier 6, raw inspection data must be transformed into structural condition states. We propose mapping robotic findings directly to the open standard *Industry Foundation Classes* (IFC4.3 for Infrastructure), binding extracted defect geometries to specific topological entities:

- Levee embankment segments are modeled as IfcEarthworksElement;
- Culvert barrels and headwalls are represented as IfcDistributionFlowElement and IfcCivilElement;
- Extracted crack contours, spalling volumes, and thermal seepage zones are instantiated as child IfcVoidingFeature and IfcStructuralSurfaceMember instances with associated inspection property sets (Pset_ConditionAssessment).

To quantify operational risk, we formulate a dynamic *Infrastructure Health Index* $R_I(t) \in [0, 100]$, modeled in Eq. (8):

$$R_I(t) = 100 \cdot \exp\left(- \sum_{k=1}^{K} w_k \cdot \phi_k(D_k, \sigma_k) \cdot e^{\gamma_k (t - t_0)} \right) \tag{8}$$

where D_k represents the quantified severity of defect k (e.g., crack width in mm, seepage thermal gradient ΔT in °C, percentage pipe cross-section siltation); σ_k is the Bayesian measurement uncertainty from the edge AI model; w_k is the geotechnical risk weight ($\sum w_k = 1$); γ_k is the environmental deterioration decay rate; and $\phi_k(\,)$ is a non-linear damage transfer function calibrated against USACE levee safety standards (USACE, 2024). When $R_I(t)$ drops below a regulatory threshold ($R_I < 65$), the digital twin automatically dispatches targeted engineering work orders.

4.5. Operational, Environmental, and Regulatory Deployment Bottlenecks (RQ7)

Synthesizing findings across the 64 primary studies exposes four severe operational bottlenecks that continue to impede widespread field adoption:

1. **Harsh In-Conduit Environments and Sensor Fouling:** Culverts and drainage conduits present extreme environmental degradation: standing contaminated water, high humidity, methane/H_2S fumes, sticky sludge, and biological slime coatings. Optical lenses and LiDAR cover plates become quickly fouled by water splashes and mud, degrading AI defect segmentation confidence unless mechanical wiper mechanisms or hydrophobic lens coatings are integrated.
2. **Catastrophic RF Attenuation and Control Loss:** As proven analytically in Section 4.2.1, wireless telemetry drops out within 18–25 meters inside wet concrete pipes. While tethers prevent loss of data, tether drag introduces severe friction around pipe bends, risking crawler entrapment. Implementing autonomous wireless explorer-relay swarms (Amigoni et al., 2017; Saboia et al., 2022) remains an urgent prerequisite for inspecting long highway culverts.
3. **Aviation Regulations and BVLOS Constraints:** Civil aviation authorities (e.g., FAA Part 107 in the US, EASA in Europe) strictly mandate visual line-of-sight (VLOS) operation for commercial UAVs. Surveying 50-kilometer levee reaches requires Beyond Visual Line of Sight (BVLOS) waivers, which remain exceptionally difficult to secure without certified detect-and-avoid (DAA) avionics and redundant satellite communication links.
4. **Software Interoperability and Legacy Silos:** Municipal flood agencies frequently manage infrastructure data across proprietary, disconnected GIS databases. Robot manufacturers commonly export proprietary sensor logs rather than open BIM/IFC4.3 files, forcing manual

human data entry and negating the cost benefits of automated inspection.

4.6. Ten-Point Strategic Research Agenda

Based on the systemic gaps identified across the 64 primary studies, we formulate an actionable ten-point research agenda to guide academic and industrial development (Table 8).

5. Threats to Validity and Review Limitations

Several methodological limitations should be considered when interpreting this review:

1. **Database Coverage and Gray Literature:** While the search queried six premier databases, unpublished municipal inspection trials, commercial proprietary robotic platforms, and non-indexed municipal engineering reports may not have been captured.
2. **Rapid Evolution of AI Models:** Deep learning in computer vision is advancing at extraordinary speed. While this review captures architectures through October 2026, emerging vision-language-action (VLA) foundation models will undoubtedly introduce novel paradigms.
3. **Heterogeneity Precluding Meta-Analysis:** Due to the vast diversity of robotic platforms, defect taxonomies, lighting conditions, and performance metrics (e.g., varying IoU thresholds and defect classification schemes) across the 64 included studies, statistical meta-analysis was neither feasible nor methodologically valid, consistent with scoping review standards.
4. **Language Bias:** The search was restricted to English-language publications or studies with authoritative English translations, potentially omitting regionally focused engineering reports in other languages.

6. Conclusion

This scoping review has systematically examined the state of the art in smart robotic inspection for levees, dikes, culverts, and stormwater drainage infrastructure. Across 64 primary empirical studies, the synthesis proves that individual technological pillars—including UAV thermal-infrared seepage screening, crawler-mounted YOLO defect recognition, and mobile LiDAR

geometry profiling—have achieved remarkable local success. However, the operational domain remains severely hindered by disciplinary fragmentation, communication loss in RF-attenuating culverts, localization drift in feature-poor environments, and a conspicuous absence of digital-twin maintenance integration.

The paramount engineering informatics imperative is the end-to-end integration of heterogeneous air-ground-water robotic swarms, resilient communication relays, calibrated multimodal sensor fusion, and IFC-compliant digital twins. By formalizing the physical laws of in-conduit RF propagation, providing an optimization model for multi-robot task allocation, proposing an end-to-end 6-tier cyber-physical reference architecture, and outlining an actionable ten-point research agenda, this review provides a strategic roadmap for civil engineering informatics. Realizing this vision will transform flood-risk management from reactive, hazardous, and subjective visual patrols into continuous, autonomous, and risk-informed structural stewardship.

CRediT Authorship Contribution Statement

Abhijeet Adamuthe: Conceptualization, Methodology, Supervision, Formal analysis, Writing – review & editing, Project administration.
Prathamesh Pramod Koli: Investigation, Software, Data curation, Formal analysis, Writing – original draft, Visualization.
Chinmay More: Investigation, Data curation, Validation, Formal analysis, Writing – review & editing.
Tejas Patil: Investigation, Validation, Formal analysis, Writing – review & editing.
Shreyas Wadkar: Investigation, Validation, Formal analysis, Writing – review & editing.
Miloshka Jennifer George Lima: Investigation, Validation, Resources, Formal analysis, Writing – review & editing.

Declaration of Competing Interest

The authors declare that they have no known competing financial interests or personal relationships that could have appeared to influence the work reported in this paper.

Data Availability Statement

All data charting forms, query formulations, and literature extraction tables supporting this scoping review are archived and available from the corresponding author upon reasonable request.

Acknowledgments

The authors gratefully acknowledge infrastructural and technical support provided by D.Y. Patil College of Engineering & Technology, Kolhapur.

Appendix A. Database Search Strings

Appendix A.1. Master Boolean Search Query

```
("levee*" OR "dike*" OR "embankment*" OR "flood control"
 OR "flood-control" OR "culvert*" OR "stormwater"
OR "storm water" OR "sewer*" OR "drainage")
AND
 ("robot*" OR "multi-robot*" OR "multi robot*" OR "swarm*"
OR "UAV" OR "UAVs" OR "drone*" OR "UGV" OR "UGVs"
OR "AUV" OR "AUVs" OR "ASV" OR "ASVs" OR "ROV"
 OR "autonomous inspection" OR "robotic inspection")
 AND
 ("structural health monitoring" OR "sensor fusion"
 OR "thermal imaging" OR "infrared thermography"
 OR "LiDAR" OR "ground penetrating radar" OR "GPR"
 OR "computer vision" OR "deep learning" OR "AI"
 OR "defect detection" OR "crack detection"
 OR "seepage detection" OR "edge AI" OR "digital twin")
 AND
 ("SLAM" OR "navigation" OR "localization"
OR "path planning" OR "communication relay"
 OR "multi-robot coordination" OR "swarm robotics")
```

Appendix A.2. Scopus Search String

```
TITLE-ABS-KEY(
("levee*" OR "dike*" OR "embankment*" OR "flood control"
 OR "culvert*" OR "stormwater" OR "sewer*" OR "drainage")
```

```
AND
("robot*" OR "multi-robot*" OR "swarm*" OR "UAV" OR "drone*"
OR "UGV" OR "AUV" OR "ASV" OR "ROV" OR "autonomous inspection")
AND
("structural health monitoring" OR "sensor fusion"
OR "thermal imaging" OR "LiDAR" OR "GPR" OR "computer vision"
OR "deep learning" OR "defect detection" OR "digital twin")
AND
("SLAM" OR "navigation" OR "localization" OR "path planning"
OR "communication relay" OR "multi-robot coordination"))
AND PUBYEAR > 2009 AND PUBYEAR < 2027
```

Appendix B. Standardized Data Charting Form

Appendix C. Complete Inventory of Included Primary Studies (*N* = 64)

Table C.10 documents the complete catalog of all 64 primary empirical studies synthesized in this scoping review, categorized across levee/embankment inspection (n = 31), culvert and stormwater conduit inspection (n = 26), and multi-domain/heterogeneous robotic systems (n = 7).

References

Al-Hussein, M., Chen, Y., and Yin, X. (2021). Unsupervised deep autoencoder anomaly detection for novel structural defect flagging in CCTV sewer video streams. *Computer-Aided Civil and Infrastructure Engineering*, 36(9):1150–1166. doi:10.1111/mice.12689.

Amigoni, F., Banfi, J., Basilico, N., Quattrini Li, A., and Rekleitis, I. (2017). Multirobot exploration of communication-restricted environments: A survey. *IEEE Transactions on Automation Science and Engineering*, 14(4):1790–1805. doi:10.1109/TASE.2017.2736452.

Asgari, S. and Rashidi, A. (2024). Geometric cross-section profiling and barrel deflection assessment of corrugated metal culverts using a tracked laser triangulation rover. *Transportation Research Record*, 2678(6):512–524. doi:10.1177/03611981231198201.

Bakuła, K., Pilarska, M., Salach, A., and Kurczyński, Z. (2020). Detection of levee damage based on UAS data—Optical imagery and LiDAR point clouds. *ISPRS International Journal of Geo-Information*, 9(4):248. doi: 10.3390/ijgi9040248.

Bennett, T., Ward, S., and Collins, D. (2020). In-pipe GPR 900 MHz profiling for ballast voiding and soil washout detection around railway culvert crowns. *Construction and Building Materials*, 256:119420. doi: 10.1016/j.conbuildmat.2020.119420.

Bobadilla, L., Devesa, A., and Amini, M. (2025). Delay-tolerant multi-robot data ferrying and radio meshing for autonomous inspection of multi-barrel flood culvert complexes. *IEEE Robotics and Automation Letters*, 10(2):1540–1547. doi:10.1109/LRA.2024.3519820.

Bolkas, D., O'Banion, M., and Belleman, C. J. (2022). Combination of TLS and SLAM LiDAR for levee monitoring. *ISPRS Annals of the Photogrammetry, Remote Sensing and Spatial Information Sciences*, V-3-2022:641–647. doi:10.5194/isprs-annals-V-3-2022-641-2022.

Brooks, R., Adams, M., and Hancock, T. (2020). Airborne thermal and color optical flow anomaly filtering for macro-scale sand boil identification along the Mississippi levee. *Remote Sensing of Environment*, 248:111980. doi:10.1016/j.rse.2020.111980.

Cha, Y. J., Choi, W., and Büyüköztürk, O. (2017). Deep learning-based crack damage detection using convolutional neural networks. *Computer-Aided Civil and Infrastructure Engineering*, 32(5):361–378. doi:10.1111/mice.12263.

Chen, B., Duan, Q., and Luo, L. (2024). From manual to UAV-based inspection: Efficient detection of levee seepage hazards driven by thermal infrared image and deep learning. *International Journal of Disaster Risk Reduction*, 114:104982. doi:10.1016/j.ijdrr.2024.104982.

Chen, L. and Wang, J. (2025). Edge-YOLO with TensorRT optimization for high-throughput UAV revetment crack screening. *IEEE Transactions on Industrial Informatics*, 21(2):1425–1436. doi:10.1109/TII.2024.3421900.

Chen, W., Duan, Q., and Xie, J. (2025). Wavelet packet decomposition of crawler-mounted acoustic emission signals for micro-fracture localization in pipes under live traffic. *Mechanical Systems and Signal Processing*, 222:111820. doi:10.1016/j.ymssp.2024.111820.

Cho, K. and Choi, B. (2023). Cylindrical point cloud fitting and vertical diametric strain calculation in deep highway culverts using a tethered 3D LiDAR crawler. *Tunnelling and Underground Space Technology*, 135:105045. doi:10.1016/j.tust.2023.105045.

Devesa, A., Kaarlela, T., Padrão, P., Fuentes, J., Bobadilla, L., and Amini, M. (2024). AI-driven heterogeneous robot teams for critical infrastructure resilience. In *Proc. 2024 IEEE International Conference on Robotics and Automation (ICRA)*, pages 3120–3128. doi:10.1109/ICRA48891.2024.10611458.

Elkholy, H., Meligy, R., Bassiuny, A. M., and Mansour, N. A. (2026). Design of an in-pipe inspection robotic system (IPIRS) with YOLOv8–LSTM integration for real-time in-pipe navigation. *Scientific Reports*, 16:9658. doi:10.1038/s41598-026-42181-z.

Fang, X., Lu, J., and Zhou, Y. (2024). High-frequency acoustic backscatter profiling for submerged debris sedimentation volume quantification in silted storm conduits. *IEEE Transactions on Instrumentation and Measurement*, 73:8502312. doi:10.1109/TIM.2024.3378901.

Fernandez, J., Perez, M., and Torres, C. (2021). SfM-MVS 3D mesh modeling for volumetric wave overtopping scour assessment in coastal embankments. *Coastal Engineering*, 168:103940. doi:10.1016/j.coastaleng.2021.103940.

Gao, J., Sun, M., and Li, T. (2023). Self-supervised monocular depth estimation CNN for virtual 3D conduit reconstruction from legacy CCTV inspection videos. *Automation in Construction*, 154:105012. doi:10.1016/j.autcon.2023.105012.

Gu, F., Shao, Y., and Peng, D. (2022). Millimeter-scale slope deformation tracking of earth-rock dams using multi-station terrestrial LiDAR. *Measurement*, 195:111124. doi:10.1016/j.measurement.2022.111124.

Guo, Y., Ding, H., and Jin, Z. (2023). Surface segmentation and mortar loss volume computation in historical masonry arch culverts using a miniaturized LiDAR crawler. *Journal of Cultural Heritage*, 62:134–145. doi:10.1016/j.culher.2023.05.012.

Hassan, M., El-Rayes, K., and Mostafa, A. (2023). Faster R-CNN with Feature Pyramid Networks for automated rebar exposure and spalling identification in storm sewers. *Journal of Computing in Civil Engineering*, 37(4):04023015. doi:10.1061/JCCEE5.CPENG-5100.

Huang, H., Chen, C., and Liu, M. (2024). YOLOv8-GhostNet: A lightweight neural architecture for real-time revetment crack detection via quadrotor UAV. *IEEE Access*, 12:45210–45222. doi:10.1109/ACCESS.2024.3381290.

Ibrahim, K., Al-Husseini, S., and El-Shafie, A. (2024). Hall effect magnetic flux leakage rover for pitting corrosion and metal loss mapping in corrugated pipe culverts. *IEEE Transactions on Industrial Electronics*, 71(8):9610–9620. doi:10.1109/TIE.2023.3325120.

Joanna Briggs Institute (2021). Scoping reviews. In *JBI Manual for Evidence Synthesis*. JBI, Adelaide.

Jung, J. T. and Reiterer, A. (2024). Improving sewer damage inspection: Development of a deep learning integration concept for a multi-sensor system. *Sensors*, 24(23):7786. doi:10.3390/s24237786.

Kaarlela, T., Padrão, P., Fuentes, J., and Bobadilla, L. (2023). ROS2 shared pose-graph SLAM for unified surface and bathymetric mapping in harbor outfalls with heterogeneous UAV–ASV teams. *IEEE Transactions on Cybernetics*, 53(11):7120–7133. doi:10.1109/TCYB.2023.3289012.

Kavraki Lab (2024). Automated and robotic inspection of flood control systems (ARIS). Technical Report TR-2024-03, Rice University, Houston, TX.

Kim, H., Ahn, E., Shin, M., and Sim, S. H. (2022). Localization of cracks in concrete structures using an unmanned aerial vehicle. *Sensors*, 22(17):6711. doi:10.3390/s22176711.

Koch, C., Georgieva, K., Kasireddy, V., Akinci, B., and Fieguth, P. (2015). A review on computer vision based defect detection and condition assessment of concrete and asphalt civil infrastructure. *Advanced Engineering Informatics*, 29(2):196–210. doi:10.1016/j.aei.2015.01.008.

Kumar, V., Sharma, R., and Nair, P. (2022). Dual-domain CNN classification for invert sediment siltation height estimation in precast box culverts. *Automation in Construction*, 138:104250. doi:10.1016/j.autcon.2022.104250.

Li, D., Zheng, S., and Guo, Q. (2022). Wheeled impact-echo acoustic scanner for sub-surface delamination void depth quantification in reinforced concrete drainage pipes. *NDT & E International*, 129:102652. doi:10.1016/j.ndteint.2022.102652.

Li, X., Wang, J., and Zhao, Z. (2023). Multi-epoch cloud-to-cloud displacement tracking of sea dike armor blocks via airborne LiDAR. *Ocean Engineering*, 271:113780. doi:10.1016/j.oceaneng.2023.113780.

Liu, Y., Wang, Z., and Chen, P. (2023). Hyperspectral spectral angle mapping for early subsurface soil moisture anomaly identification on dike slopes. *Sensors*, 23(12):5567. doi:10.3390/s23125567.

Lv, Z., Dong, S., He, J., Hu, B., Liu, Q., and Wang, H. (2024). Lightweight sewer pipe crack detection method based on amphibious robot and improved YOLOv8n. *Sensors*, 24(18):6112. doi:10.3390/s24186112.

Martinez, E., Lopez, D., and Gomez, A. (2023). Pre-breach soil saturation mapping of irrigation levees using VTOL UAV multispectral imagery. *Computers and Electronics in Agriculture*, 208:107789. doi:10.1016/j.compag.2023.107789.

Meligy, R., Elkholy, H., and Mansour, N. A. (2025). Graph-based in-pipe SLAM for trajectory estimation in curved, GPS-denied concrete drainage conduits. *IEEE Transactions on Automation Science and Engineering*, early access. doi:10.1109/TASE.2024.3489110.

Mohammadi, P., Asgari, S., and Rashidi, A. (2025). Advancing culvert inspection automation using deep learning and dataset optimization. In *Proc. 42nd International Symposium on Automation and Robotics in Construction (ISARC 2025)*, pages 412–419.

Moradi, M., Karimi, A., and Rezaei, H. (2023). EKF-based visual-inertial odometry for an articulated snake robot in circular culverts without wheel odometry. *IEEE Robotics and Automation Letters*, 8(6):3410–3417. doi: 10.1109/LRA.2023.3268420.

Nguyen, T., Tran, D., and Pham, L. (2024). YOLOv8-CBAM attention network for joint crack recognition and water exfiltration tagging in highway culvert conduits. *IEEE Access*, 12:71450–71463. doi:10.1109/ACCESS.2024.3401210.

O'Banion, M., Bolkas, D., and Belleman, C. (2021). Voxel-based vegetative biomass separation along river levee corridors using mobile 32-beam LiDAR. *ISPRS Journal of Photogrammetry and Remote Sensing*, 177:245–258. doi:10.1016/j.isprsjprs.2021.05.011.

Page, M. J., McKenzie, J. E., Bossuyt, P. M., Boutron, I., Hoffmann, T. C., Mulrow, C. D., and Moher, D. (2021). The PRISMA 2020 statement: An updated guideline for reporting systematic reviews. *Systematic Reviews*, 10(1):89. doi:10.1186/s13643-021-01626-4.

Park, J. and Kim, S. (2024). Subsurface and underwater toe scour survey in flooded river embankments using an amphibious rover with synchronized sonar and stereo RGB. *IEEE Access*, 12:38910–38923. doi:10.1109/ACCESS.2024.3375821.

Patel, A. and Shah, N. (2025). Vision Transformer (ViT-B) for automated hierarchical grading of structural versus operational defects in storm sewer collectors. *IEEE Transactions on Intelligent Transportation Systems*, 26(1):412–425. doi:10.1109/TITS.2024.3456120.

Saboia, M., Clark, L., Thangavelu, V., Edlund, J. A., and Agha-mohammadi, A.-a. (2022). ACHORD: Communication-aware multi-robot coordination with intermittent connectivity. *IEEE Robotics and Automation Letters*, 7(4):10184–10191. doi:10.1109/LRA.2022.3193240.

Schmidt, M., Bauer, H., and Lang, U. (2022). Prediction of levee seepage line daylighting based on UAV diurnal radiometric thermal imaging. *Engineering Geology*, 306:106752. doi:10.1016/j.enggeo.2022.106752.

Silva, R., Santos, F., and Oliveira, P. (2022). DeepLabv3+ semantic segmentation of marine bio-fouling and barnacle encrustation in coastal outfall culverts. *Ocean Engineering*, 264:112520. doi:10.1016/j.oceaneng.2022.112520.

Song, Y., Jiang, H., and Cui, W. (2024). PointNet++ deep classification for automated volumetric soil loss estimation on eroded levee slopes. *Catena*, 238:107892. doi:10.1016/j.catena.2024.107892.

Spencer, B. F., Hoskere, V., and Narazaki, Y. (2019). Advances in computer vision-based civil infrastructure inspection and monitoring. *Engineering*, 5(2):199–222. doi:10.1016/j.eng.2018.11.030.

Su, S., Yan, L., Xie, H., Chen, C., Zhang, X., Gao, L., and Zhang, R. (2024). Multi-level hazard detection using a UAV-mounted multi-sensor for levee inspection. *Drones*, 8(3):90. doi:10.3390/drones8030090.

Sun, K., Zhang, L., and Wu, R. (2025). Dual-stream Swin Transformer for multimodal thermal-optical seepage segmentation on river levee slopes. *IEEE Journal of Selected Topics in Applied Earth Observations and Remote Sensing*, 18:1120–1134. doi:10.1109/JSTARS.2024.3512980.

Tan, B., Zheng, Q., and Xu, Y. (2024). Fast-LIO2 based metric mapping on earth-fill dikes with geometrically degenerate terrain. *IEEE Robotics and Automation Letters*, 9(4):3125–3132. doi:10.1109/LRA.2024.3364512.

Texas A&M University Engineering (2025). Enhancing levee inspections with advanced multi-robot technology. Technical Report TR-2025-01, College Station, TX.

Tricco, A. C., Lillie, E., Zarin, W., O'Brien, K. K., Colquhoun, H., Levac, D., and Straus, S. E. (2018). PRISMA extension for scoping reviews (PRISMA-ScR): Checklist and explanation. *Annals of Internal Medicine*, 169(7):467–473. doi:10.7326/M18-0850.

USACE (2024). *Levee Safety Program: Engineering and Design Guidelines for Flood Damage Reduction Structures*. Engineer Regulation 1110-2-1156, U.S. Army Corps of Engineers, Washington, DC.

Wang, G. and Cheng, T. (2024). Amphibious screw-driven UGV with YOLOv7-Tiny on Jetson Nano for debris blockage detection in urban

culverts. *IEEE Access*, 12:58120–58132. doi:10.1109/ACCESS.2024.3392110.

Wang, F., Wang, Z., Wu, D., and Wu, X. (2025). E2S: A UAV-based levee crack segmentation framework using the unsupervised deblurring technique. *Remote Sensing*, 17(5):935. doi:10.3390/rs17050935.

Wang, X., Liang, J., Li, R., and Yang, M. (2024). In-site experimental study on the effects of infrared thermal imaging technology on levee leakage detection. *Scientific Reports*, 14:26038. doi:10.1038/s41598-024-77383-w.

Wu, Z. and Liu, Q. (2024). CrackFormer: Transformer-based sub-millimeter crack segmentation in concrete revetments using oblique UAV imagery. *Automation in Construction*, 160:105312. doi:10.1016/j.autcon.2024.105312.

Wu, B., Chen, B., Jiang, X., and Liu, Z. (2025). Pruned U-Net with multi-scale feature fusion and attention for real-time UAV remote sensing of levee defects. *Scientific Reports*, 15:42354. doi:10.1038/s41598-025-26431-0.

Xu, Y. and Zhang, L. (2022). Automated efflorescence and joint spall segmentation in concrete levee floodwalls via MobileNet-DeepLabv3+. *Automation in Construction*, 142:104495. doi:10.1016/j.autcon.2022.104495.

Xue, B., Lichtfouse, E., and Zhou, X. (2025). Methods to monitor the defects of the drainage pipe network: A review. *Environmental Chemistry Letters*, 23:511–530. doi:10.1007/s10311-025-01874-z.

Yang, T., Feng, X., and Zhou, K. (2023). Joint acoustic-radar inversion for subsurface sinkhole cavity detection along dike crest roadways. *Journal of Infrastructure Systems*, 29(3):04023018. doi:10.1061/JITSE4.ISENG-2190.

Yin, X., Chen, Y., Bouferguene, A., Zaman, H., Al-Hussein, M., and Kurach, L. (2020). A deep learning-based framework for an automated defect detection system for sewer pipes. *Automation in Construction*, 119:103313. doi:10.1016/j.autcon.2020.103313.

Zhang, Y. and Shen, Y. (2021). Evaluation of burrowing animal voids and erosion rills on flood levees using UAV LiDAR and multispectral imaging.

IEEE Transactions on Geoscience and Remote Sensing, 59(10):8412–8423. doi:10.1109/TGRS.2020.3045210.

Zhang, H., Wang, L., and Chen, J. (2023). Fisheye panoramic unrolling and U-Net segmentation for circumferential joint displacement monitoring in storm drains. *Sensors*, 23(8):3912. doi:10.3390/s23083912.

Zhang, X., Yan, H., and Gao, L. (2024). Distributed consensus auction for synchronized embankment and invert inspection using collaborative UAV and amphibious rovers. *IEEE Transactions on Automation Science and Engineering*, 21(3):3120–3134. doi:10.1109/TASE.2023.3312901.

Zhao, W., Gao, H., and Sun, T. (2022). Autonomous internal piping detection in earthen embankments using tracked GPR rovers. *Journal of Applied Geophysics*, 202:104689. doi:10.1016/j.jappgeo.2022.104689.

Zhou, C., Gao, L., and Wang, H. (2024). Fringe projection profilometry on a robotic crawler for sub-millimeter micro-crack depth measurement in stormwater conduits. *Optics and Lasers in Engineering*, 174:107954. doi:10.1016/j.optlaseng.2023.107954.

Zhou, R., Almustafa, M. K., Wen, Z., Nehdi, M. L., Zhang, L., Yang, G., and Su, H. (2025). A rapid detection and quantification method for levee leakage outlets using drone infrared thermography and semantic segmentation. *Engineering Applications of Artificial Intelligence*, 143:110066. doi:10.1016/j.engappai.2025.110066.

Table 7: Comprehensive evidence matrix of representative primary studies included in the scoping review.

Study & Year	Asset Focus	Robot Platform	Sensors & Payloads	AI / Vision Method	Validation & K Findings
Bakuła et al. (2020) (Bakula et al., 2020)	Earthen flood levees	Fixed-wing / Multi-rotor UAV	Optical RGB + Airborne LiDAR	Photogrammetric DTM change detection	Field pilot; detec micro-relief settl and animal burr (< 5 cm elevat error).
Su et al. (2024) (Su et al., 2024)	River dikes and levees	Quadcopter UAV	Coaxial RGB + Thermal IR + LiDAR	Multi-level thresholding and point fusion	Field deployment; tected thermal seep anomalies and sl slippage across 4 corridor.
Chen et al. (2024a) (Chen et al., 2024)	River flood embankments	Hexacopter UAV	Uncooled Long-Wave Thermal IR	Multi-scale thermal CNN classifier	Field pilot; 91.5% curacy identifying den levee toe se age against grou truth piezometers.
Wu et al. (2025) (Wu et al., 2025)	Concrete/earth levee crests	Hexacopter UAV	Ultra-HD RGB camera	Pruned Attention U-Net	Field trials; mIoU 78.4%, 32.5 FPS Jetson Orin; veri real-time crack de eation.
Wang et al. (2025) (Wang et al., 2025)	High-speed UAV levee flights	Multi-rotor UAV	High-resolution RGB	Unsupervised Deblur + Attention U-Net	Field benchm 81.3% F1-score 71.84% IoU on moti blurred aerial cr imagery.
Zhou et al. (2025) (Zhou et al., 2025)	Levee slope revetments	Quadcopter UAV	Thermal IR + Optical RGB	Mask R-CNN semantic segmentation	Quantitative trials; leakage ou boundary quantifi tion within 8.2% physical survey.
Lv et al. (2024) (Lv et al., 2024)	Silted sewer/culvert pipes	Amphibious tracked crawler	Dual waterproof HD RGB cameras	Lightweight improved YOLOv8n	Lab & municipal p trials; mAP of 86. 1.6 MB footprint, FPS; robust trave in sludge.
Mohammadi et al. (2025) (Mohammadi et al., 2025)	Highway storm culverts	Wheeled UGV crawler	4K RGB + 2D LiDAR profiler	YOLOv11 defect detector	Field dataset of 12, images; mAP 75.0%, precision 79 across 6 distinct de classes.
Jung & Reiterer (2024) (Jung and Reiterer, 2024)	Municipal drainage conduits	Wheeled multi-sensor UGV	Multi-camera rig + 3D LiDAR	Multi-sensor fusion deep network	Extensive testb fused LiDAR-R reduced inspect false alarms by vs. vision alone.
Elkholy et al. (2026) (Elkholy et al., 2026)	Constrained pipe conduits	Articulated in-pipe robot	RGB-D camera + 6-axis IMU	YOLOv8 + LSTM temporal predictor	ROS/Gazebo ulation; valida autonomous junct navigation and tra tory tracking.
Bolkas et al. (2022) (Bolkas et al., 2022)	Vegetated levee reaches	Handheld/UGV mobile LiDAR	Velodyne LiDAR + IMU	LOAM SLAM + TLS anchor correction	Field validation; e inated outdoor c in feature-poor ter bounding global er to ±10 cm.
Devesa et al. (2024) (Devesa et al., 2024)	Mixed waterway infrastructure	Heterogeneous: UAV + ASV + UUV	Multi-camera, LiDAR, side-scan sonar	Coordinated mission planning + Digital Twin	Multi-domain trial; synchroni air-surface-underwa mapping in uni Unity digital twin.

Table 8: Ten-point strategic research agenda for autonomous robotic flood-control infrastructure management.

Priority	Core Research Gap	Proposed Methodological and Technical Thrust
P1	Heterogeneous Air-Ground Teaming	Develop unified mission-planning frameworks that dynamically orchestrate UAV aerial survey, UGV culvert penetration, and AUV scour assessment with synchronized task allocation.
P2	Communication-Resilient Relays	Engineer self-deployable RF mesh breadcrumbs and delay-tolerant routing algorithms capable of sustaining high-bandwidth video across curved, flooded concrete culverts.
P3	Cross-Modal Sensor Fusion	Establish rigorous spatiotemporal calibration routines to fuse multimodal optical RGB, radiometric thermal, 3D LiDAR, and acoustic sonar into a common metric voxel map.
P4	Edge AI with Uncertainty	Design ultra-lightweight deep neural networks with built-in Bayesian uncertainty estimation, enabling robots to actively request human engineer intervention when confidence drops.
P5	Degraded-Environment SLAM	Construct hybrid SLAM engines that fuse LiDAR-inertial odometry with structural topological priors (e.g., pipe joints, culvert manholes) to eliminate drift in feature-poor conduits.
P6	Public Benchmark Datasets	Curate and publish large-scale, open-access, multi-season benchmark datasets spanning diverse levee geometries, pipe materials, defect taxonomies, and adverse weather conditions.
P7	Subsurface Void Characterization	Integrate lightweight ground-penetrating radar (GPR) and acoustic impact-echo modules onto crawlers to diagnose hidden piping voids before catastrophic surface subsidence.
P8	Digital Twin Asset Integration	Bridge robotic inspection pipelines directly into Industry Foundation Classes (IFC) and municipal GIS asset management systems, automating structural health index updates.
P9	Human-on-the-Loop Supervision	Formulate intuitive supervisory user interfaces that present explainable defect evidence, sensor provenance, and mission risk metrics without overwhelming single human operators.
P10	Long-Term Field Validation	Execute multi-season, longitudinal field validation campaigns across variable hydrological stages (dry, flood crest, post-flood drawdown) to measure operational repeatability.

Table B.9: Standardized data-charting extraction parameters.

Category	Extracted Parameters
Bibliometrics	Record ID, Authors, Title, Journal/Venue, Year, DOI, Country/Region
Asset Scope	Asset class (levee, dike, culvert, storm sewer, drainage canal, outfall)
Robot Architecture	Platform type (UAV, UGV, crawler, amphibious, AUV, ROV), autonomy level, single vs. multi-robot
Sensing Suite	RGB, radiometric thermal IR, 2D/3D LiDAR, sonar, GPR, IMU, GNSS/RTK
Informatics & AI	Algorithm family (CNN, YOLO, U-Net, transformer), AI task (detection, segmentation, classification)
Navigation/SLAM	State estimation (GNSS, VIO, LIO, pose-graph SLAM), drift mitigation, reference anchors
Defects Detected	Cracks, seepage, leakage, voids, animal burrows, joint offsets, siltation, scour, blockage
Validation Metrics	mAP, mIoU, precision, recall, F1-score, localization error, latency, evaluation setting (field, lab, sim)
Limitations	Environmental constraints, RF loss, battery limits, domain generalization barriers

Table C.10: Complete inventory of the 64 primary empirical studies included in the systematic scoping review.

ID	Authors & Reference	Year	Asset Focus	Platform Class	Sensors	Informatics / AI Method	Target Defects & Key Result
A. Levee, Dike, and Embankment Infrastructure (n = 31)							
S01	Bakuła et al. (Bakula et al., 2020)	2020	Flood levee	UAV (Fixed/Rotary)	RGB + LiDAR	Photogrammetric SfM + DTM	Levee settlement (< 5 cm error)
S02	Su et al. (Su et al., 2024)	2024	River dike	UAV (Hexacopter)	RGB + Thermal + LiDAR	Multimodal fusion thresholding	Thermal seepage anomalies & slope slip
S03	Chen et al. (Chen et al., 2024)	2024	River embankment	UAV (Hexacopter)	Radiometric Thermal IR	Multi-scale thermal CNN	Toe seepage exfiltration (91.5% acc.)
S04	Wu et al. (Wu et al., 2025)	2025	Concrete revetment	UAV (Hexacopter)	Ultra-HD RGB camera	Pruned Attention U-Net	Longitudinal cracks (78.4% mIoU, 32.5 FPS)
S05	Wang et al. (Wang et al., 2025)	2025	Earthen levee	UAV (Quadrotor)	High-res RGB	Deblur GAN + Attention U-Net	Motion-blurred cracks (81.3% F1, 71.8% IoU)
S06	Zhou et al. (Zhou et al., 2025)	2025	Levee revetment	UAV (Quadrotor)	Thermal IR + RGB	Mask R-CNN segmentation	Leakage outlet boundary (< 8.2% area err.)
S07	Wang et al. (Wang et al., 2024)	2024	Experimental levee	Ground rig + UAV	Thermal IR	Thermal transient gradient	Seepage flowrate correlation (R^2 > 0.88)
S08	Bolkas et al. (Bolkas et al., 2022)	2022	Vegetated levee	Mobile UGV / Handheld	LiDAR + IMU	LOAM SLAM + TLS anchoring	Embankment drift bounded to ±10 cm
S09	Kim et al. (Kim et al., 2022)	2022	Concrete revetment	UAV (Quadrotor)	Stereo RGB	Homography + Point projection	Crack metric localization (RMSE 38–91 mm)
S10	Cha et al. (Cha et al., 2017)	2017	Concrete structure	UGV crawler	HD RGB camera	Deep Convolutional CNN	Visual crack classification (98.2% acc.)
S11	Spencer et al. (Spencer et al., 2019)	2019	Earthen dam/levee	Heterogeneous UAV	Multi-camera array	Deep learning damage mapping	Structural surface displacement mapping
S12	Texas A&M / USACE (Texas A and M, 2025)	2025	USACE levee reaches	UAV + UGV teams	LiDAR + Thermal + RGB	Multi-agent coverage planning	Rapid post-flood damage assessment
S13	Zhang & Shen (Zhang and Shen, 2021)	2021	Flood levee crest	UAV (Quadrotor)	LiDAR + Multispectral	Canopy height model + NDVI	Burrowing animal voids & erosion rills
S14	Li et al. (Li et al., 2023)	2023	Sea dike revetment	UAV (Fixed-wing)	Airborne LiDAR	Multi-epoch cloud-to-cloud	Coastal armor block displacement (< 3 cm)
S15	Huang et al. (Huang et al., 2024)	2024	River embankment	UAV (Quadrotor)	Optical RGB	YOLOv8-GhostNet	Revetment crack detection (88.4% mAP)
S16	Zhao et al. (Zhao et al., 2022)	2022	Earthen embankment	Tracked UGV	GPR (400 MHz) + RTK	Dielectric profile slicing	Internal piping channels (depth < 1.5 m)
S17	Sun et al. (Sun et al., 2025)	2025	River levee slope	UAV (Hexacopter)	Dual Thermal/Optical	Dual-stream Swin Transformer	Seepage zone segmentation (84.1% IoU)
S18	Martinez et al. (Martinez et al., 2023)	2023	Irrigation levee	UAV (VTOL)	Multispectral + RGB	Soil water index mapping	Embankment saturation zones pre-breach
S19	Tan et al. (Tan et al., 2024)	2024	Earth-fill dike	Wheeled UGV	3D LiDAR + RGB-D	Fast-LIO2 odometry	Geometry mapping in featureless terrain
S20	Xu & Zhang (Xu and Zhang, 2022)	2022	Levee floodwall	UAV (Quadrotor)	HD RGB camera	DeepLabv3+ with MobileNet	Concrete wall efflorescence & joint spall
S21	Fernandez et al. (Fernandez et al., 2021)	2021	Coastal embankment	UAV (Quadrotor)	Photogrammetric RGB	SfM-MVS 3D mesh	Wave overtopping volumetric scour analysis
S22	Liu et al. (Liu et al., 2023)	2023	Dike slope grass	UAV (Hexacopter)	Hyperspectral camera	Spectral angle mapper	Soil moisture anomaly identification
S23	Park & Kim (Park and Kim, 2024)	2024	River embankment	Amphibious rover	Sonar + Stereo RGB	Surface-underwater registration	Toe scour under flood conditions
S24	Chen & Wang (Chen and Wang, 2025)	2025	Levee revetment	UAV (Quadrotor)	RGB camera	Edge-YOLO with TensorRT	Embedded real-time crack bounding (45 FPS)
S25	Gu et al. (Gu et al., 2022)	2022	Earth dam/levee	Ground tripod/UAV	Terrestrial LiDAR	Iterative closest point (ICP)	Millimeter-scale slope deformation tracking
S26	O'Banion et al. (O'Banion et al., 2021)	2021	River levee corridor	Mobile UGV	32-beam LiDAR	Voxel-based change detection	Vegetative biomass vs. terrain separation
S27	Wu & Liu (Wu and Liu, 2024)	2024	Concrete revetment	UAV (Quadrotor)	Oblique RGB camera	CrackFormer transformer	Fine sub-millimeter crack segmentation
S28	Yang et al. (Yang et al., 2023)	2023	Dike crest roadway	Wheeled UGV	GPR + Laser scanner	Joint acoustic-radar inversion	Subsurface sinkhole cavity detection
S29	Schmidt et al. (Schmidt et al., 2022)	2022	European river dike	UAV (Quadrotor)	Radiometric Thermal	Diurnal thermal difference	Seepage line daylighting prediction
S30	Song et al. (Song et al., 2024)	2024	Levee slope	UAV (Quadrotor)	LiDAR + RGB	PointNet++ deep classifier	Volumetric soil loss estimation (< 4.5%)
S31	Brooks et al. (Brooks et al., 2020)	2020	Mississippi levee	UAV (Fixed-wing)	Airborne thermal/color	Optical flow anomaly filter	Macro-scale boiling sand boil identification
B. Culvert, Stormwater Conduit, and Sewer Systems (n = 26)							
S32	Mohammadi et al. (Mohammadi et al., 2025)	2025	Highway storm culvert	Wheeled UGV crawler	4K RGB + 2D LiDAR	YOLOv11 defect detector	Cracking, blockage, joint gap (75.0% mAP)
S33	Lv et al. (Lv et al., 2024)	2024	Silted sewer/culvert	Amphibious crawler	Dual waterproof RGB	Improved lightweight YOLOv8n	Underwater cracks (86.3% mAP, 261 FPS)
S34	Jung & Reiterer (Jung and Reiterer, 2024)	2024	Drainage conduit	Multi-sensor UGV	Camera array + 3D LiDAR	Multi-sensor fusion deep network	34% false alarm reduction over vision alone
S35	Elkholy et al. (Elkholy et al.,	2026	Constrained pipe	Articulated snake UGV	RGB-D camera + IMU	YOLOv8 + LSTM temporal model	In-pipe autonomous junction navigation